

PHASE II RESEARCH PLAN

REV 12/01

Specific Aims

Phase I feasibility successfully demonstrated the construction and evaluation of a functional, bench top analyzer prototype based on a **CCD (charge coupled device)** camera and a multi-channel, bioluminescence biosensor. The analyzer prototype and associated biosensor were capable of quantifying ATP analyte samples simultaneously from six discrete channels each having a 20 μL volume. The bench top prototype was constructed from commercially available components (CCD camera, laptop computer, collection optics) and machined parts.

This Phase II proposal addresses the continued development and evaluation of a miniaturized and fully functional engineering prototype based on a CCD detector and a **personal digital assistant (PDA)** hand held computer. The second emphasis will be on the refinement and further miniaturization of the biosensor design for better compatibility with the analyzer and application to small ($<100 \mu\text{L}$) blood samples. TABLE I in Section B provides a device specification that will serve as a target to focus the development effort for both analyzer and biosensor. The goal of this project is to develop an inexpensive, reliable, accurate handheld analyzer and associated disposable biosensor that can be used in point of care or home health care environments to simultaneously quantify multiple analytes of clinical relevance. The target analytes for this will be creatinine, lactate, ATP, and NADH. The Specific Aims of the proposed two year development project are:

Review the options available for micro-controllers, PDAs, software development tools, and CCD chips. Make the appropriate selections and order. Review, revise, and update the product specification and user interface as necessary and revisit the design parameters based upon any changes made. Create a design specification.

Mechanical Design: Design and layout the optical system with an emphasis on size, cost and image quality

using CAD tracing software. Design the overall device package and have the first models machined from

plastic. Design the sample strip (biosensor) chamber for reproducible insertion and light tightness. Also

allocate volume for battery power and electronic circuitry.

3. *Electrical and Software Design:* Design analog and digital circuit boards, create design schematics and circuit

board layout. Evaluate the various options for system power considering size, power density and cost after the

power needs have been determined. Design and write all of the software necessary to control the CCD chip

voltages, read the chip, process and store the data, operate the user interface, control all power distribution and

download the data to the modem or wireless connection of the personal digital assistant.

4. Construct two copies of the first prototype. One copy will be evaluated for

mechanical fit and then for initial

performance testing. The second copy will be used for software evaluation, refinement and de-bugging.

5. Based upon the evaluation results in #4, implement any necessary design, parts and materials changes and

have a second generation of three engineering prototypes constructed. One prototype will be used for

electronics evaluation and enhancement. The second one will be used as a platform for continued software

development and refinement. The third prototype will be evaluated for performance (sensitivity, accuracy, signal

stability over the specified operating time, temperature, and humidity ranges) and mechanical robustness.

6. Redesign the biosensor prototype to address issues of additional miniaturization, reduced cost, incorporation of

a blood separation membrane, and compatibility with analyzer design. Also increase the individual, separate analyte channels from six to twelve and minimize the total required blood sample volume.

7. Based upon the previous test and evaluation results construct three more additional, fully functional engineering

prototypes and evaluate the performance of the hardware and the software. These will be considered to be the

final project deliverables in addition to all of the design and development documentation for both the device

prototype and the associated disposable biosensor strip.

Obtain a commercial or prototype **CMOS (complementary metal oxide)** imaging camera and evaluate it's

performance in comparison to the ST7I camera used in the Phase I prototype. If the results are encouraging

build the CMOS camera into an engineering prototype. The primary metrics will be signal, noise, minimum

threshold for all four analytes, linearity, and signal stability.

Background, Significance, Relevant Experience and System Specifications

Protein Solutions, Inc. (PSI) is focused on the development of quantitative, multi-analyte, luminescence-based, biosensors that are easy-to-use, inexpensive, and disposable. Such sensors would be used both in point-of-care testing and eventually for self-monitoring in the home environment. We are developing a "Metabolite Chip" - a multi-channel, biosensor capable of quantitatively measuring dozens of metabolites simultaneously. Such a chip would literally "image" metabolism and give a quantitative "picture" of the metabolic status of an individual [Andrade, et al. 1999]. The ability to simultaneously quantify many parameters of metabolism will be a great asset to research as well as to clinical and preventative medicine, with a major benefit being reduced healthcare cost. The biosensor and its associated analytical measuring device could quantify a wide range of carbohydrates, amino acids, vitamins, and other low molecular weight molecules of relevance to clinical medicine, detection and management of inborn errors of metabolism, nutrition, sports medicine and related areas such as the biotechnology and bio-process industries. Other multi-channel luminescence based sensors for quantitatively analyzing a spectrum of therapeutic drugs and proteins is our second goal. It would be highly desirable to

monitor the levels of therapeutic drugs that have narrow ranges of effectiveness and toxicity. One classic example is cyclosporin. The biochemistry basis for such assays will be a variant of an enzyme linked, luminescent immunoassay approach [REFERENCE], but again, the output signal for quantification purposes would be light.

Multi-channel biosensors for a family of diagnostically related analytes (metabolites, proteins, drugs, etc.) could be mass produced for a few dollars each. Less than 100 microliters (μL) of blood would be required for operation (0.5 to 2.0 μL of blood plasma per channel) and this could easily be obtained via a painless micro-lancet stick on the finger tip. The patient would not need to interpret all of the data generated, but would merely download the test results to a remote hospital or clinic data base for storage, additional analysis and review by their clinician. The download could be accomplished with an integral modem or a wireless connection.

Our luminescent approach to analysis has three main components - (1) the biochemistry for analyte specificity and transduction to light that is proportional to analyte concentration, (2) the disposable biosensor which contains the reagents and receives the blood sample, and (3) the analytical device which quantifies the luminescence, stores the result, interfaces to the user and downloads results to a remote patient data base via wireless or modem communications. **The focus of this Phase II effort is the development of the analytical device and a compatible biosensor platform.** The analytical approach is based on a charge coupled device (CCD) sensor in combination with an optical system that images the array of luminescent biosensor channels onto the CCD. We envision the device to be battery powered, inexpensive and handheld. CCD based luminometers do exist for high volume clinical chemistry labs, but they are very large and expensive and cost many thousands of dollars [REFERENCE].

Until recently, our approach to signal transduction has been exclusively bioluminescence, however, we are now investigating chemiluminescent immunoassay approaches for application to proteins and drugs. Firefly bioluminescence is based on the enzyme (luciferase) catalyzed oxidation of luciferin utilizing ATP as a highly specific co-reactant [REFERENCE]. Magnesium ion is also a necessary luciferase co-factor. Marine bacterial bioluminescence is closely coupled to an NADH-dependent enzyme reaction and is catalyzed by a bacterial luciferase [REFERENCE]. These reactions are highly sensitive to and quantitative for ATP and NADH over a concentration range of more than five orders of magnitude [REFERENCE]. Since all of metabolic biochemistry depends upon ATP or NADH, literally hundreds of metabolic analytes linked to ATP and NADH can be monitored via a bioluminescence approach.

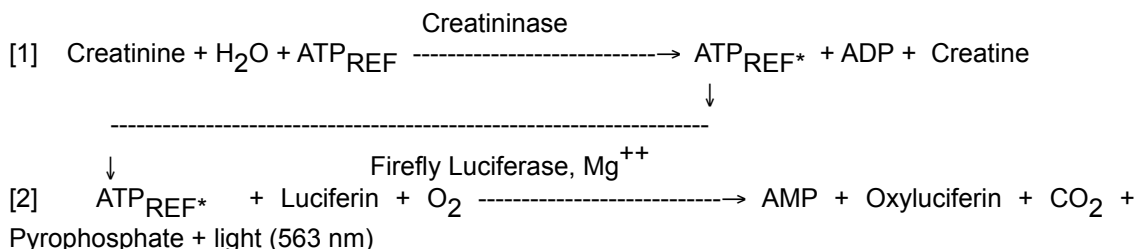
Although bioluminescence analysis is well known and has been used regularly in research and in analytical and clinical laboratories, it has not been widely applied outside those specialty areas for several reasons. First, the exquisite sensitivity for very low ATP concentrations has encouraged the application of the technique to those problems where such sensitivity is needed. Thus, it has acquired the reputation of an ultra-sensitive technique and has not been seriously considered for the measurement of analytes in the 1-1,000 micro-molar range. Second, the luciferases and other reagents involved have developed a reputation of being somewhat labile, unstable, and difficult to utilize. Additionally, sources of various luciferases have, until recently, been of questionable purity, variable activity and considerable expense.

We are convinced that both ATP-based firefly luminescence and NADH-based bacterial bioluminescence can serve as highly specific and sensitive means of monitoring the molecules of metabolism. During the last four years we have developed both the ATP [REFERENCE] and NADH [REFERENCE] biochemistries which minimize the problems noted above. Our approach has been based on the following considerations. First, the biotechnology community knows how to express, produce, and purify proteins via simple organism cultures and processes. Indeed, recombinant firefly and bacterial luciferases have been known for some time now and both are commercially available with much more consistency in purity and activity for a reasonable cost [REFERENCE Promega and Sigma]. Second, the biotechnology and protein pharmaceutical industries have learned how to formulate, passivate, store, and reconstitute labile proteins and enzymes with considerable retention of activity [Fagain, Carpenter]. We have addressed the instability of firefly and bacterial luciferase using our experience, understanding, and control of the denaturation of proteins at interfaces and in solution [Wang]. Third, a reaction which produces photons against a dark signal background has the advantage that no light source is required, as is the case with fluorescence, UV-Vis, Raman, and IR spectroscopies. This lowers cost and raises reliability, but more importantly the minimum detection threshold **signal to noise (S/N)** is improved because there is no noise associated with a large optical background noise. Fourth,

one does not require electrodes with their tendencies to become contaminated or to participate in side reactions, as in the case of much of analytical electro-chemistry.

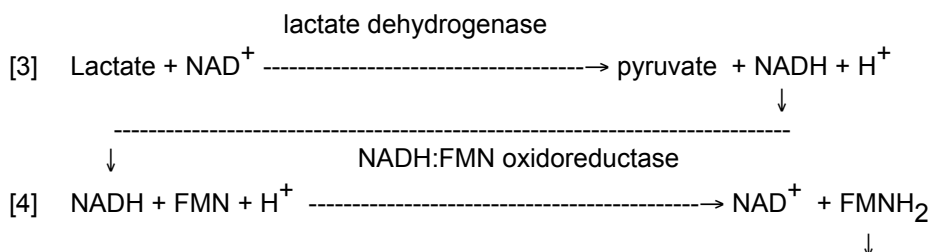
Most of our progress to date involves measuring and quantifying bioluminescence linked to specific biochemical reactions with ATP or NADH as intermediates. We have developed biosensor chemistries for phenylalanine [Min, 1999], galactose [Eu, 1999], and creatinine/creatine [SBIR Grant#]. Good progress has also been made via this Phase I SBIR to develop the CCD camera based analyzer and the associated multi-channel biosensor. Our bioluminescence intensity-based approach uses the absolute intensity of the bioluminescence, which can be made directly or inversely proportional to substrate concentration. The more classical analyzer is generally a photomultiplier tube (PMT) based photon counting luminometer which can accurately measure ATP levels down to less than one femto-molar [REFERENCE]. While our CCD camera based luminometer can simultaneously quantify analytes in the various channels of the biosensor the sensitivity of the CCD is about 100-1,000 times less than a PMT which only has single channel capability. However, all of the molecules of interest to us exist in the low nanomolar to low millimolar range which is sufficient to be detected by the CCD approach. At this time, our CCD system can detect ATP down to the 10 nano-molar level and this should certainly improve by at least a factor of ten with the optimization of our biosensor design and higher activity luciferases. This should make the luminescence based quantification of proteins and drugs in the low nano-molar range possible.

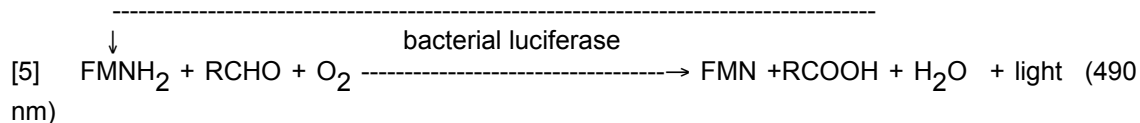
Reactions [1-2] illustrate the biochemical approach for the detection of creatinine and ATP. Residual ATP in a sample can be determined using Reaction 2 and firefly luciferase. The determination of creatinine employs a homogeneous assay where both Reactions 1 and 2 are proceeding simultaneously. This is possible because firefly luciferase is a much slower enzyme than creatininase. This is essentially an ATP depletion assay where added ATP_{REF} is depleted to ATP_{REF}* via Reaction 1. Reaction 2 is then used to determine the amount of ATP left.



In this homogeneous ATP depletion assay reference ATP (ATP_{REF}), Mg⁺⁺, luciferin, O₂, creatininase and luciferase are added reagents. The original amount of creatinine analyte is inversely proportional to the amount of signal arising from the ATP not consumed by Reaction 1 at some time, T, after the reaction begins. Thus, there is an inverse relationship between the amount of creatinine and the bioluminescent light signal measured at the λ_{MAX} of 563 nm for firefly luciferase. Other representative analytes that can be measured via this approach are: glucose, pyruvate, creatine, ammonia, urea and riboflavin if the appropriate enzymes for Reaction 1 above are employed.

Reactions 3-5 below can be employed to measure a variety of amino acids and as well as alcohol and lactate. Reactions 4 and 5 can be used to assay NADH. The use of NAD and lactate dehydrogenase in Reaction 3 below provide for the assay of lactate.





Equations 3-5 represent an NADH/FMNH₂ production reaction where the added reagents are nicotinamide adenine dinucleotide (NAD), flavin mononucleotide (FMN), long chain aldehyde (RCHO, i.e., dodecanal), and the three enzymes noted above. The amount of bioluminescence produced ($\lambda_{\text{MAX}} = 490 \text{ nm}$) is directly proportional to amount of L-lactate present in the sample.

The focus of the research and development effort proposed for Phase II is to develop a fully functional engineering prototype analyzer and associated multi-channel biosensor platform for ATP, NADH, creatinine and lactate based on biochemical reactions 1-5 above. The development, optimization and stabilization of the biochemistries for these particular analytes is beyond the scope of this work and is actually the current focus of other specific funding including, but not limited to NIH SBIR grants.

In the short term, we anticipate that the materials cost of such an analyzer will be \$300 - \$400 and the disposable will be about \$10. However, our goal is to produce disposable, multi-channel biosensors for a few dollars [Andrade, et al., 1999] and analyzers costing about \$200. The latter should be possible when the expensive CCD chips (\$70 in quantity) are superceded by CMOS image sensors costing only a few dollars [REFERENCE].

Table I below summarizes the specifications which will guide the design and development effort for the CCD based luminescence analyzer and associated biosensor.

TABLE I Device Specifications for CCD Multi-Channel Analyzer and Associated Biosensor

Maximum Dimensions:	Analyzer:	Length: 125 mm, Width: 75 mm, Thickness: 25 mm
	Biosensor:	Length: 35 mm, Width: 12.5 mm, Thickness: 2 mm
Maximum Weight:	Analyzer:	250 grams (8.8 oz)
Power Supply:	Disposable batteries with sufficient capacity to conduct one test per day for one year.	
Operating Temperature:	Analyzer and biosensor 50°F to 95°F (10°C to 35°C)	
Storage Temperature:	Analyzer: -20°F to 130°F (-29°C to 54°C) and biosensor: -29°C to 35°C	
Operating Humidity:	Analyzer: 10 to 90 % RH (non-condensing)	
Memory:	Sufficient to store 100 test results and associated dates and times.	
User Interface:	51 mm x 51 mm monochrome liquid crystal display, audible beeper or alarm with three buttons (On/Off, Scroll/Select, and Enter) or touch screen via PDA computer.	
Mechanical Robustness:	Capable of surviving a 30 G deceleration.	
Communications:	Accessory modem for data download, new software updates and remote diagnostics plus RS232 port link to computer or personal	

digital assistant.

Analytes and Channels: Twelve channels: four analytes plus background and calibration channels.

Sample: A maximum 100 μ L whole blood sample which yields ~ 40 μ L of plasma via a polymeric blood separation membrane.

Hematocrit Range: 25 to 60 %

Calibration: Plasma equivalent concentration values for all analytes.

On sensor calibration for all four analytes, or if necessary with a small liquid calibration solution.

Analysis Range: Four amino acids via ATP and/or NADH intermediates: 1 micro-molar to 10 milli-molar

Accuracy: \pm 10 percent of full scale over any single decade range over the complete

analysis range.

Reliability: No moving mechanical parts, i.e., no fans, shutters, gears, etc. and a minimum MTBF target of 72 months

Warranty: Three years except for batteries and obvious mechanical abuse in excess of

30 G's deceleration or exposure to liquids.

Materials Cost: Analyzer: \$300 - \$400 range with individual part quantities of 10,000

Biosensor: Less than \$10 in quantities of 10,000

Phase I Final Report

Phase I Project Details

a. Project beginning date: 07-01-98
04-30-99

b. Project ending date:

Key Personnel:

<u>Name</u>	<u>Title</u>	<u>Service Period</u>	<u>H o u r s</u>
<u>Contributed</u>			
R. Van Wagenen 820	Principal Investigator	07-01-98 to 04-30-99	
C.-Y. Wang	Research Scientist	07-01-98 to 07-30-98*	45
R. Scheer	Research Scientist	07-01-98 to 09-30-98*	30
M. Hammer 568	Lab Technician	07-01-98 to 04-30-99	
J.D. Andrade	Technical Advisor	07-01-98 to 04-30-99	30

* Dr. Sheer left the company on August 12, 1998 and Dr. Wang left the company on September 30, 1998.

d. Publications and Patents: At this time (November, '99), there are NO publications, manuscripts accepted for publication, patents granted or pending, patent disclosures, invention reports or other publicly available printed material resulting from the Phase I effort.

e. Summary of Original Phase I Specific Aims: The goals of the Phase I project were: (1) Construct a functional, bench top prototype bioluminescence analyzer using commercially available components, i.e., a charge coupled device (CCD) imaging camera, an imaging lens, and a lap top computer for data acquisition, analysis, and data display. (2) Evaluate the CCD based prototype using commercially available luminescence standards in terms of absolute sensitivity threshold and signal linearity AND validate a signal modeling equation which relates the luminescence standard flux to signal detected with the CCD. (3) Convert the existing single channel ATP biosensor design to a smaller four-channel design which can be directly inserted into the analyzer. (4) Evaluate the analyzer prototype and four-channel ATP biosensor in terms of: (a) minimum detection threshold, (b) signal intensity as a function of time as a measure of system stability and reproducibility, and (c) accuracy and precision. Three different measurement modalities were to be compared and contrasted, i.e., (aa) Direct analytical determination of ATP analyte concentration based on prototype signal intensity. (bb) CCD imaging of the spatial distribution of the bioluminescence much like a glowing thermometer in the dark (see original Phase I proposal) with the distribution of the bioluminescence being directly proportional to the analyte concentration, and (cc) a combination of the two (aa and bb) approaches.

f. Changes to Phase I Specific Aims: There were three changes to the original work plan summarized above. First, as a prelude to purchasing the actual CCD camera, the specifications, cost and availability of cameras from several vendors were reviewed. Second, three CCD cameras were extensively evaluated before one was selected for incorporation into the prototype. Third, Specific Aims 4bb and 4cc noted above were not investigated because, in our opinion, a spatial distribution of bioluminescence determined via the CCD camera would greatly complicate the biochemistry and sample distribution design which would have to be incorporated into the biosensor. Also, the spatial distribution approach required a larger biosensor area and a concomitantly greater amount of expensive reagents, i.e., luciferin and luciferase. Finally, we felt this approach would greatly complicate the data analysis. These three changes are reflected in the sequence of activities that are reported next.

Phase I Results (sequentially by Revised Specific Aims)

Review of CCD Camera Specifications

Technical literature was reviewed for the following CCD camera systems: Santa Barbara Instruments Group (SBIG) Models ST-6, ST-7 and ST-8, Meade Pictor Model 216XT, Celestron PixCel Model 255, Apogee Instruments Model AM16, and Starlight Express Model MX516. All of these camera systems are relatively low cost devices that are used by amateur astronomers. Very high performance CCD camera systems costing tens of thousands of dollars are available for research purposes, but such systems and the CCD chips inside them would never be cost effective for the kind of inexpensive handheld device envisioned for our application. Refer to device specifications in TABLE I, Section B.

The primary factors considered in the selection of cameras for in house evaluation were: (1) CCD chip read noise, dark current, quantum efficiency at 560 nm, pixel full well capacity AND (2) camera size, the availability of a 16 bit A/D, cost, availability (some cameras were back ordered for 6-12 months) and software user interface features. The three cameras selected for evaluation were the ST6A, ST7I, and MX516. TABLE II on the next page summarizes the relevant features of these cameras. The ST7I camera was chosen primarily because it contained the Kodak KAF-0400 CCD chip. This chip was designed by Kodak to be used in low cost consumer electronic cameras and to have very low dark current at room temperature [REFERENCE]. The MX516 camera was selected primarily because of its small size, low cost (~\$1,100), acceptable read noise and dark current (based on specifications) and absence of moving parts (no cooling fan or mechanical shutter). All three cameras were controlled using software operating under Microsoft Windows 95.

Evaluation of Three CCD Camera Systems

Evaluation of the three CCD camera systems required a lens to collect the luminescence and image it onto the CCD. A 28 mm focal length, f/2.8 Olympus Zuiko wide angle camera lens was used with the ST6A and ST7i. The MX516 camera used a 12 mm focal length, f/1.2 Computar lens. Three Biolink™ luminous reference standards (Biolink Technology, Ltd.) were employed for most of the camera evaluations. These standards consist of hermetically sealed glass vials containing tritium gas and a phosphor.

TABLE II. A Summary of CCD Chip and Camera Specifications

<u>Parameter</u>	<u>ST6A Camera</u>	<u>ST7I Camera</u>	<u>MX516 Camera</u>
Camera Vendor	SBIG ¹	SBIG ¹	
Starlight Xpress ²			
Read Noise	30 e ⁻	15 e ⁻	25 e ⁻

Dark Current	<30 e ⁻ /s (-20°C)	<0.5 e ⁻ /s (0°C)	
0.05 e ⁻ /s (-10°C)			
A/D	16 bit	16 bit	16 bit
QE	50 % @ 550 nm	43% @ 550 nm	
50% @ 550 nm			
Cooling	One Stage TE ³	Two stage TE ³	One Stage TE ³
	cooler + fan	cooler + fan	No fan
Dimensions	151 mm diameter	128 x 128 mm	
50 mm diameter			
	71 mm thick	71 mm thick	
100 mm long			
Shutter	Electromechanical	Electromechanical	
None ⁴			
Chip Vendor	Texas Instruments	Kodak	Sony
Chip Model	TC 241	KAF-0400 ⁵	
ICX055 ⁴			
Pixel Size	23 X 27 μm ⁶	9.0 x 9.0 μm	9.8 x
12.6 μm			
Pixel Array	242 x 375 pixels	510 x 765 pixels	256
x500 pixels			
Total Pixels	90,750	390,150	
128,000			
Chip Dimensions	6.5 x 8.6 mm	4.6 x 6.9 mm	3.6 x
4.9 mm			
Chip Full Well Capacity	400,000 e ⁻	40,000 e ⁻	
120,000 e ⁻			

Notes: 1. Santa Barbara Instrument Group, Santa Barbara, CA.
Functional Design & Engineering Ltd., Berkshire England.

Solid State Thermo-electric (TE) Cooler.

This is an inter-line transfer chip designed originally for a camcorder.

Chip designed to be a true phase CCD for very low dark current and low cost chip for consumer electronic cameras.

6. Two $13.5 \times 27 \mu\text{m}$ pixels are electronically binned to yield a $23 \times 27 \mu$ pixel, but the original chip aspect ratio causes a distorted image.

scintillator [Leaback]. The vials are sealed in an aluminum block and the windowed end opposite the phosphor provides the photon flux which is varied via the incorporation of neutral density filters of differing transmittance in each of the five channels. FIGURE 1 shows both a CCD room light view and a dark view (60 s exposure) of the three Biolink™ dna 17 ,07 :# laireS) sdradnats ecnerefer .9991 ,enuJ rof deificeps slennahc 51 eht fo hcae morf xulf notohp eht dna (28

Thermal Performance

Both the ST6A and ST7I cameras had integrated thermo-electric (TE) coolers heat sunk to a finned aluminum heat exchanger which comprised part of the camera housing. A fan on the housing enhanced convective cooling. The ST6A camera contained the Texas Instruments TC241 CCD chip and could be cooled to -20°C for optimal performance, but this required two TE coolers linked in series. The ST7I camera contained the Kodak KAF-0400 CCD chip which only had to be cooled to 0°C using one TE cooler. The use of a TE cooler, fan and heat exchanger added considerably to the size of the camera head and the power consumption. The CCD temperature of the SBIG cameras could be set, controlled and monitored continuously via an on-chip thermal sensor that was linked to both the user interface and a feedback loop to the cooler power supply controller. The MX516 camera was half the size of the ST6A and ST7I because, in part, it had a single TE cooler and no cooling fan. There was no CCD chip temperature monitoring capability for the MX516. The manufacturer indicated that chip cool down from 24°C required about 20 minutes to an equilibrium operating temperature of -10°C .

FIGURE 2 illustrates the thermal performance for the ST6A and ST7I operated at chip temperatures of -20°C and 0°C , respectively. Note that the cooling capacity of the ST6A was considerably greater than the ST7I. The ST6A cooled down from 26°C to -20°C in 3-4 minutes while the ST7I required 12 minutes to attain it's equilibrium operating temperature of 0°C . At equilibrium, both cameras were capable of maintaining a stable chip temperature. The temperature variation on the ST7I ($\pm 0.2^{\circ}\text{C}$) looks larger than the ST6A ($< \pm 0.1^{\circ}\text{C}$) but may, in fact, only be due to the resolution of the thermcouple temperature sensor linked to the Kodak chip. When the thermo-electric coolers are turned off the chips warm up to room temperature over a 10 to 20 minute period. The ST7I reaches a temperature somewhat greater than room temperature (29°C) because some of the heat from the hot side of the TE cooler conducts back through the cooler and into the chip whereas this does not occur

as much through the two series linked TE coolers of the ST6A.

Conclusion: Both the ST6A and ST7I cameras had very adequate short term thermal performance in terms of cool down and temperature stability at operating temperature. The MX516 camera was inferior because there no hardware or software capability to set the CCD chip temperature or provide any indication of what the actual chip temperature really was at any given time.

Dark Frames and Bias Frames

CCD cameras are superb devices for quantitative imaging [REFERENCE]. However, the photosites (pixels) which comprise the CCD array are not all identical. There are very sensitive “hot” pixels, minimally sensitive “cool” pixels, a wide variation of pixels between the two extremes, and occasionally some “dead” pixels that do not respond at all to light. There can also be progressive variations of pixel sensitivity across the CCD chip and artifact patterns resulting from defects in the optical system (dust, optical vignetting, etc.). Consequently, there is often a big difference between the desired calibrated image that accurately reflects the light source intensity and the initial raw image obtained directly from the camera.

The raw CCD image is a composite of: (1) the signal from the luminous source, (2) the thermal signal accumulated in each pixel during the exposure time, (3) the bias signal composed of (a) the amplifier zero-point offset (if any), (b) random readout noise from the on-chip amplifier, and (c) other camera electronics noise, and (4) extraneous signal response arising from pixel-to-pixel sensitivity variations, stray light, and image artifacts such as dust shadows and image vignetting arising from the optics. A dark frame is generally taken immediately before or after the raw image frame. The dark frame exposure is the same time duration as the raw image frame. It contains the thermal and bias signals and is thus equal to the sum of the thermal frame and bias frame. The dark frame is then subtracted from the raw signal frame to produce a partially corrected image. For precise calibration the partially corrected image is divided by a flat-field frame that corrects for pixel-to-pixel sensitivity variations and optical artifacts. In summary:

Desired Calibrated Image = [Raw Image – Bias Image – Thermal Image] / [Flat Field Frame] OR

Desired Calibrated Image = [Raw Image – Dark Frame] / [Flat Field Frame]

The resulting calibrated image then accurately represents the number of signal photons that fell on the various pixels of the CCD chip. The fully calibrated image has a normalized sensitivity to light at every pixel in the image and it is free from thermal and bias signals. However, the calibrated image does retain residual, random noise from the bias, thermal and flat-field correction frames. Thus, it is still important to minimize these three factors by minimizing bias and thermal signals and by taking multiple correction frames and averaging them.

There is one other random source of signal and noise background – cosmic ray collisions with some of the pixels in the chip. This is generally a rare event for CCD chips, occurring about once every thirty minutes for small 1/4” chips. When a cosmic ray collides with a CCD one or more pixels will exhibit extremely high signals above background, often the pixel(s) will saturate. A study was conducted to assess the frequency of this effect. All three cameras were run for six 5 minute integrations in the dark. The six frames were co-added together to give a cumulative signal representing 30 minutes of dark integration. Each frame was analyzed for pixels having extremely high count levels (greater than 10,000 counts per pixel). None were observed for any

of the three cameras confirming minimal cosmic ray influence.

The magnitude of the electronic offset, read noise and electronics noise for each camera was measured by determining a bias frame for each of the three cameras. None of the cameras had the ability to take a zero integration time exposure bias frame. However, the dark frame is the sum of the bias frame and the thermal frame and the bias frame is independent of exposure time while the thermal frame intensity increases directly as a function of exposure time. So one simply takes two dark frames at the same chip operating temperature – one frame for 10 seconds exposure and a second frame having twice the exposure time, i.e., 20 seconds. The bias frame is then obtained by subtracting the long dark exposure frame (20 s) from two times the short exposure frame (10 s). This was done for each camera and the average pixel intensity averaged over 18 positions on the image were determined. The average pixel intensity at each of the 18 positions was, in turn, an average of a 31 x 31 pixel array, i.e., 961 pixels. The results are presented in TABLE III below.

TABLE III Average Bias Frame Determinations for Three CCD Cameras

<u>Parameter</u>	<u>ST6A</u>	<u>ST7I</u>	<u>MX516</u>	<u>Units</u>
Mean Bias Frame Signal	130	110	1,654	Digital Counts/ pixel
$\pm 2 \sigma$ Standard Deviation	± 23	± 3	± 113	Digital Counts/pixel

The manufacturers of the ST6A and ST7I incorporate a amplifier zero point offset bias voltage on the CCD chip that produces 100 digital counts/pixel in the bias frame. The MX516 has no zero point offset bias so its bias frame consists of only the amplifier readout signal and associated noise and other miscellaneous noise from the camera electronics. Consequently, we can see from TABLE III above that the amplifier readout and electronics noise is: 30, 10, and 1,654 digital counts/pixel for the ST6A, ST7I and MX516, respectively. According to the manufacturers specifications the read noise for the MX516 should be about the same as the ST6A, but it appears to be 55 times greater!

Note the different 2σ standard deviations in TABLE III. These are averages of eighteen 31 x 31 pixel arrays, six each taken on the top tier, the middle tier, and the bottom tier of the bias frame. Bias frames for each of the three cameras show a brightness (signal) gradient from top to bottom because during the finite time required to read the CCD (several seconds) the thermal noise continues to build up in the pixels which have not yet been read. Consequently, the last rows of pixels, i.e., the bottom pixels in the image appear to have a bit more signal than the top pixels. This is indicated as a wider standard deviation for the ST6A versus the ST7I where the ST7I has both lower dark thermal current and a faster chip read time.

The dark signal performance characteristics for each of the three cameras was determined by taking dark exposures as a function of integration time with the cameras operating at their optimal temperature (-20°C for the ST6A, 0°C for the ST7I and approximately -10°C for the MX516) and then subtracting the

amplifier offset bias signal of 100 digital counts for the ST6A and the ST7I and 0 digital counts for the MX516. The results are shown in FIGURE 3 and the regression analysis results and calculated dark current are shown in TABLE IV below.

TABLE IV Thermal Dark Signal Performance for Three CCD Cameras

<u>Parameter</u> <u>Units</u>	<u>ST7I</u>	<u>ST6A</u>	<u>MX516</u>	
Correlation Coefficient, r	0.9992		0.9995	
Slope, m	0.188	2.600	0.23	thermal
y-intercept b	3.4	27.2	1,692	bias
Calculated Thermal Coefficient photo-electrons/s	0.4	17.4	*	
Specified Thermal Coefficient photo-electrons/s	0.5	< 30		0 . 0 5

Note: * The photo-electrons/digital count were not supplied by the manufacturer of the MX516.

Notice in TABLE IV that the y-intercepts for the ST7I and ST6A (3 and 27 digital counts, respectively) represent the amount of bias remaining because the bias offset counts (100) were already subtracted out. These experimental numbers compare reasonably well with those determined previously for the bias counts arising from the sum of the on chip amplifier and associated electronics noise, i.e., 10 and 30, respectively from TABLE III. The slope of the line, m, represents the thermal dark signal coefficient, i.e., 0.19, 2.60, and 0.23 digital counts per pixel per second for the ST7I, ST6A, and MX516, respectively. To convert pixel digital counts per second to photo-electrons per pixel per second one must multiply these slopes by the following conversion factors for the ST6A and ST7I cameras: 6.7 and 2.3 photo-electrons per digital count, respectively. The results are: 17.4 photo-electrons per pixel per second for the ST6A and 0.4 photo-electrons per pixel per second for the ST7I. This is in good agreement with the specified values of <30 and 0.5 for the ST6A and ST7I, respectively. See TABLE II.

Conclusion: The ST7I is superior to the ST6A and highly superior to the MX516 in terms of bias frame signal and noise and thermal dark current. Cosmic ray events do not seem to be a significant issue for any of the cameras, i.e. none were detected for integration periods of 30 minutes.

Response Linearity

The three cameras were evaluated for response linearity using Biolink™† channel # 82-1 as a constant photon flux light source. See Section C.2.b for information on the Biolink™档 standards. Each camera was turned on and the CCD chip sensor was set to the appropriate operating temperature (MX516 had no user selectable temperature) using the Windows 95 software user interface on the laptop computer. Camera integration times were varied from 1 s

incrementally up to 120 s so that an increasing number of photons were collected in each of the CCD pixel wells comprising the image of the source. At some cumulative amount of total integrated signal each pixel saturates.

FIGURE 4 illustrates the linearity and saturation signal level for each of the CCD cameras. The slopes of the linear regions are different due to somewhat different optical parameters in the collection lenses, i.e., the effective aperture is different due to the focal length difference and/or the f # setting used for each lens. There are two important conclusions. First, all three cameras exhibit excellent linearity in their respective linear regions. The linear regression correlation coefficients, r , are better than 0.9998 for each camera. Second, each camera has a fairly sharp inflection region followed by a plateau in signal response even though the total photon flux continues to increase with increasing exposure time, i.e., the pixels are saturated. The saturation levels for the three cameras are: 64,000, 56,000 and 47,000 analog/digital count units for the MX516, ST7I and ST6A, respectively. The plateau saturation levels are a function of the full well capacity for the pixels of each camera and the camera electronics gain. These are factors that are unique to each of the three camera designs.

Conclusion: All three cameras have excellent response linearity in their linear ranges and knowledge of the saturation levels for each camera provides an upper acceptable limit on total integrated counts per pixel for quantitative purposes.

Short Term and Long Term Stability

The three cameras were evaluated for short-term stability (1hr.) and long-term stability (10hr.) using the Biolink™ † Channel # 82-1 reference light standard as a constant photon flux light source. See Section C.2.b for information about the Biolink™ 桃 standards. Each camera was turned on and the CCD chip was set to the appropriate operating temperature (MX516 had no user selectable temperature) using the Windows 95 user interface on the laptop computer. After 30 minutes of warm up (primarily to account for the unknown equilibrium temperature of the MX516) the first 20 second camera exposure was taken, dark frame subtracted, downloaded and stored. Additional identical exposures were taken at ten minute periods over one hour and then hourly over for 10 hours.

Results for all three cameras are shown in FIGURE 5. The average pixel signal is an average of 961 pixels centered at the same position on the image of the light standard. TABLE V summarizes the analytical results.

TABLE V Means, Standard Deviations, Coefficients of Variation, and Linear Regression Slopes for Short and Long Term Signal Stability of the Three CCD Cameras.

<u>Parameter</u> <u>Units</u>	<u>ST6A</u>	<u>ST7I</u>	<u>MX516</u>
Operating Temperature setting 10°C °C	-20°C	0°C	~
<u>One Hour Stability Study</u>			
Mean Signal, x 11,828* Digital counts	8,074	9,552	
± 2 Sd. Dev.(±2σ)	5	11	151

Digital counts			
Coefficient of Variation ($[2\sigma/x]100$)	$\pm 0.06\%$	$\pm 0.12\%$	
$\pm 1.28\%$ Percent			
Linear slope	-1.3	-2.3	-24.0
Pixel counts/hr			
<u>Ten Hour Stability Study</u>			
Mean Signal, x	8,071	9,510	
13,591* Digital counts			
± 2 Sd. Dev. ($\pm 2\sigma$)	11	57	237
Digital counts			
Coefficient of Variation ($[2\sigma/x]100$)	$\pm 0.14\%$	$\pm 0.60\%$	
$\pm 1.74\%$ Percent			
Linear slope (pixel counts/hr)	-1.4	-9.3	+8.0
Pixel counts/hr			

NOTE: * Optical conditions were changed between the one and ten hour stability runs for the MX516.

Conclusion: The ST6A camera was clearly superior to the ST7I and MX516 cameras in terms of overall signal stability during both one and ten hour periods. The two stage, series TE cooler in the ST6A camera had more thermal control capacity than the single stage TE coolers of the ST7I and MX516.

Measurement Precision

Each camera was employed to measure the light intensity from the brightest Biolink™ 捡 Channel (82-1). The amount of light reaching the CCD chip was controlled by adjusting the variable aperture in the collection lens and/or the integration time. Dark frame background subtraction was done after each integration to eliminate the thermal signal, but its associated noise could not be subtracted out so integration times were kept short (0.1s to 10 s) to minimize thermal signal and noise. Ten integrations were performed at increasing photon flux levels corresponding to approximately 100, 1,000, 10,000 and 40,000 digital counts per pixel. Means and two sigma standard deviations were calculated as well as signal:noise ratios and coefficients of variation based on $[\pm 2 \sigma / \text{mean}]$. Results are summarized in TABLE VI below.

TABLE VI Measurement Precision as Coefficient of Variation for the three CCD Cameras

Mean Signal	Noise or Precision as $\pm 2 \sigma$	Signal:Noise	
Coefficient of Variation			
<u>$[\text{Digital Counts/Pixel}]$</u>	<u>Standard Deviation</u>	<u>$\pm 2\sigma / \text{mean}$</u>	<u>$[\pm 2\sigma /$</u>
<u>$\text{mean}] \times 100$</u>			

~ 100	~10	~10:1	
~10.0 %			
~ 1,000	~25	~40:1	~ 2 . 5
%			
~ 10,000	~110	~90:1	
~1.1 %			
~ 40,000	~280	~143:1	~ 0 . 7
%			

Conclusion: The S/N ratio improves as the square root of the increase in either total mean signal or counting time. For instance, increasing the total integration time by 100 or the total integrated signal counts by a factor of 10,000/100 = 100 improves the signal to noise ratio by about the square root of 100. In our case this was 90/10 = 9. The coefficient of variation improves by the same factor of 9. This is typical of Poisson counting statistics for randomly occurring quantum events such as photon flux. Measurement precision was found to be virtually the same for each of the three cameras despite the considerably higher on-chip amplifier noise of the MX516 camera.

Minimum Detection Threshold Sensitivity

A relative comparison of sensitivity detection threshold was made for all three CCD cameras using the Biolink™ † reference standards # 70 and #71. The two standards were photographed in the dark with integration times ranging from 10-600 seconds. All three cameras were able to detect Channels 70-1, 71-1, 70-2 and 71-2 with a 10 second exposure. None of the cameras was able to detect Channel 70-5 with a 10 minute exposure. The noise associated with the cumulative thermal signal plus the read noise from the on-chip amplifier always compromised the ability to detect the fifth channel. Figure 6A shows a room light CCD picture of the two standards and FIGURE 6B shows a 600 second integration in the dark using the ST7I. Note in this Figure that channels 1 through 3 are easily visible for both standards and that channel 70-4 is just marginally detectable with a 600 integration. The Biolink #70 data (Biolink #71 was essentially the same) for the three cameras is summarized in TABLE VII below for the 300 and 600 second integration times.

TABLE VII Signal Levels for Three CCD Cameras as a Function of Source Intensity and Integration Time

Biolink™ 漢 MX516	Photon flux MX516	ST6A	ST6A	ST7I	ST7I
<u>Channel</u>	<u>[Photon/s/sr]</u>	<u>300 s</u>	<u>600 s</u>	<u>300 s</u>	<u>600 s</u>
<u>300 s</u>	<u>600 s</u>				
70-1	7.00 E 7	10,413±465	20,453±944	1,907±180	3,815±204
13,334	25,426				

70-2	1.20 E 7	2,217± 62	4,174± 54	366± 13	639± 21
4,647	7,550				
70-3	1.15 E 6	314± 26	375± 43	129± 8	158± 12
1,941	2,300				
70-4	1.09 E 5	123± 28	105± 10	106± 7	110± 9
1,623	1,754 ± ~ 100				
70-5	1.10 E 4	119± 17	100± 9	102± 7	103± 9
1,600	1,650 ± ~ 100				
Background*	0	100± 10	100± 10	100± 10	100± 10
1,650	1,650 ± ~ 100				

* The background signals and associated noise at zero photon flux are the sum of the offset bias voltage signal (100 c/pixel for the ST6A and ST7I and 0 for the MX516), the on-chip amplifier noise and signal and the thermal dark signal accumulated over 300 or 600 seconds of integration.

The data in TABLE VII and the image frames (not shown for the ST6A and MX516) indicate that all three cameras were able to detect $\sim 1 \times 10^6$ photons/s/sterradian (channel 70-3) with a 300 second integration. However, even a 600 second integration is not sufficient to attain a statistically significant level of detection to $\sim 1 \times 10^5$ photons/s/sterradian (Channel 70-4). This is indicated by the detection threshold line in TABLE VII. The noise associated with the on-chip amplifier and camera electronics of the MX516 (~ 100 digital counts/pixel) suggests that it could not detect channel 70-4 and is somewhat inferior to the other two cameras.

Conclusion: The ST6A and ST7I cameras appear to be comparable in detection threshold and given that the image frames for both cameras do show Channel #70-4 we conclude that with more comprehensive signal analysis it should be possible to detect $\sim 100,000$ photons/s/sterradian with both of these cameras and a 600 second signal integration.

Camera Selection Rationale

The MX516 was easily the least desirable of the three camera options. This was primarily due to the lack of quantitative CCD chip temperature indication or temperature control and the poor software user interface which did not provide for easy background subtraction, pixel sampling, data processing or image manipulation. Also, while the MX516 seemed to have a low thermal dark signal coefficient it had a high amplifier read signal and associated noise. The ST7I camera was selected for the prototype primarily because of its very low thermal dark current, low on chip amplifier signal and acceptable thermal control performance. While the ST7I did cost about 50 percent more than the ST6A, it offered the best long term potential for low signal detection and cost reduction via the Kodak KAF-0400 chip. Finally, the ST7I was packaged more compactly than the ST6A.

Construction of Functional Bench Top Prototype Analyzer and Four Channel Biosensor

Before the ST7I could be incorporated into a functional prototype the final choice on luminescence collection optics had to be made. The primary issues were to: (1) minimize the

working distance between the image plane of the CCD and the luminescence source on the biosensor so the prototype was as small as possible, (2) maximize the amount of light collected from the channels of the biosensor, and (3) completely image the active area of the biosensor (8.5 mm x 13.5 mm) onto the CCD chip (4.6 mm x 6.9 mm) with as little image distortion as possible.

The following three Olympus camera lenses were evaluated for this task: (1) 50 mm focal length, f/1.8 lens, (2) 28 mm focal length, f/2.8 wide angle lens, and (3) 50 mm focal length, f/3.5 macro lens. Three extension rings (12 mm, 20 mm and 36 mm) were also evaluated in conjunction with the lenses in order to minimize the working distance between the biosensor and the collection lenses.

For each lens and ring combination (including the no ring scenario) a preliminary assessment was made to determine if the four channels of the biosensor could be properly imaged onto the CCD chip with good focus and depth of field for various combinations of lens focus setting and working distance. The 20 mm and 36 mm extension rings were quickly disqualified. Even though their working distance was very small (a few mm) the depth of focus was extremely small (sub-millimeter) and the object (biosensor) could not be completely imaged onto the CCD. More comprehensive evaluations with the 12 mm extension ring and the three lenses led to the best combination of lens, ring, focus setting, depth of focus field, and working distance for proper imaging and minimum optical working distance. The optimal configuration was a 12 mm extension ring in combination with the 28 mm focal length, wide angle lens set to a focus of 1.25 feet and a working distance between the camera base and biosensor of 140 mm.

A photograph of the bench top prototype based on this optical design is shown in FIGURE 7. On the right is the AC/DC transformer for the camera electronics. It is rather large, primarily because of the high power draw required by the single stage thermo-electric cooler that cools the CCD chip. The laptop computer (Winbook FX, 133 MHz) is on the left. On the display is an image of bioluminescence from four of the channels of the ATP biosensor. In the center of the photograph is the prototype analyzer comprised of a black anodized aluminum cylinder mounted on top of the ST71 camera head. The cylinder serves to position the biosensor 140 mm from the base of the camera. The top center of the black cylinder has a 25 mm diameter windowed aperture which serves to partially support the biosensor and allow luminescence to reach the collection lens. The top surface of the window is not visible because a black anodized aluminum cap covers the sample chamber to keep stray light from reaching the collection lens.

The prototype multi-channel ATP biosensor is also shown at the bottom of FIGURE 7. The body of the biosensor is made of black acrylic with dimensions: 50 mm long, 12.5 mm wide and 6 mm thick. The four channels each 2 mm in diameter penetrate the thickness of the acrylic and are arranged in a square array spaced 3 mm center-to-center. Each round channel is 2 mm diameter and contains a multi-fiber wick produced by Filtrona Richmond (Richmond, VA). The wicks are comprised of heat and pressure bonded polyester fibers (Transorb[®] 9 R-19363 wicks) treated with 0.1% Triton X-100 detergent. The polyester wicks serve to precisely draw a given volume of sample into them via capillarity. The wicks have a geometrical volume of 18.8 mm^3 or $18.8 \mu\text{L}$ and a void volume of about 60% so each wick holds $12 \mu\text{L}$ of sample ($2 \mu\text{L}/\text{mm}$). A circular paper (Schleicher & Schuell S&S[®] 903) pad 8 mm in diameter overlays the channel

array and serves as a sample application target and reservoir for liquid sample before it is wicked into the fibers.

Evaluation of Prototype Analyzer and Modeling Equation

The ST7i cooling fan is located on the backside of the camera head and the camera is oriented vertically to look up at the sample positioned above it. Consequently, the fan could not draw cooling air with the prototype supported by a flat surface. The solution was to attach three small rubber feet around the bottom circumference of the camera head. This provided 12 mm of space below the camera for cooling air to flow. A short study was conducted to determine if there was enough air flow to keep the CCD chip at 0°C with <80% of the maximum power available for the TE cooler (as recommended by the manufacturer). The prototype was operated with a cooler temperature of 0°C as a function of ambient air temperature between 20°C and 28°C while the percentage of power to the chip was monitored. It was found that for ambient air temperatures of 24°C or less the air flow was sufficient to keep the thermo-electric cooler power at <80% of maximum.

Because the Kodak KAF-0400 CCD chip was designed to have an ultra-low thermal dark current we conducted studies to determine just how sensitive it was at 25°C in contrast to 0°C. Biolink™ siht rof desu erew 28 dna 07 sdradnatS desu erew 3-07 dna ,2-07 ,1-07 ,5-28 ,3-28 slennahC .yduts nosirapmoc evitaler a dennaps yeht dna xulf suonimul mrofinu yllaitaps a detibihxe yeht esuaceb degami dna edis yb edis decalp erew sdradnats ehT .tuptuo thgil fo egnar ediw dluoc sdradnats htob ni slennahc eht lla taht os gnir noisnetxe mm 21 eht tuohtiw detcartbus dnuorgkcab lamreht krad laudividni neT .pihc eht otno degami eb htiw ksid ot derots dna nekat yllaitneuqes erew noitarud sdnoces 06 fo serusopxe muirbiliuqe retfa dna C°0 ot delooc neht saw pihc ehT .C°52 ta pihc DCC eht 06 fo serusopxe detcartbus dnuorgkcab lamreht krad erom net deniatta saw eht fo eno morf langis ehT .ksid ot derots dna nekat yllaitneuqes erew sdnoces net eht fo hcae rof dedrocer saw slennahc evif eht fo hcae fo retneC eht ta slexip erew snoitaived dradnats σ2 dna snaeM .C°0 dna C°52 ta serusopxe evif eht rof noitairav tnemerusaem ro noisicerp eht tneserper esehT .denimreted neht saw ssecorp emas ehT .C°52 dna C°0 htob ta seitisnetni lennahc tnereffid ehT .emit noitargetni dnoCes 006 a htiw serutarepmet htob ta semit net detaeper .IIIV ELBAT ni nwohs era stluser

TABLE VIII ST7I Camera Sensitivity for 0°C and 25°C with both 60 and 600 second integration periods.

	Specified	60 seconds	60 seconds	600 seconds	600seconds
	Luminous	CCD Chip	CCD Chip	CCD Chip	CCD Chip
		@ 0°C	@ 25°C	@ 0°C	
Biolink					
@25°C					
Channel	Intensity*	Mean ± 2σ [#]	Mean ± 2σ [#]	Mean ± 2σ [#]	Mean ± 2σ [#]

82-3	8.60 E 8	763.9 ± 2.1	756.3 ± 4.2		
70-1	7.00 E 7	274.9 ± 1.6	274.8 ± 3.9		
70-2	1.20 E 7	133.4 ± 1.5	134.0 ± 4.0		
82-5	3.66 E 6	105.2 ± 1.6	105.7 ± 4.3	141.4 ± 1.5	141.9 ± 3.6
70-3	1.15 E 6	104.6 ± 1.5	104.9 ± 3.4	137.5 ± 2.0	137.3 ± 4.2
Background	0	101.4 ± 1.5	101.9 ± 3.8	104.8 ± 1.7	104.0 ± 3.0

* Photons/s/sterradian

Based on N=10 samples

The results in TABLE VIII suggest that at a CCD chip temperature of 0°C and 60 seconds integration there is a statistically significant difference between a background zero flux and a signal flux of 1.2×10^6 photons/s/sterradian. This detection threshold of 1.2×10^6 photons/s/sterradian improves in significance with a 600 second integration. This is consistent with the results in TABLE V. However, at a chip temperature of 25°C and 60 s integration the statistically significant difference between signal and background zero flux occurs at 1.2×10^7 photons/s/sterradian. Consequently, we conclude that by operating the CCD at room temperature we give up a factor of ten in minimum detection threshold for a 60 s integration. It may however, not be quite this bad because the data in TABLE VIII were based upon measurements from a single pixel in the Biolink™ 散 channel image. In reality, there are many pixels that comprise the image and if the cumulative signal in all of the pixels are considered the counting statistics improve considerably. Referring to TABLE VIII again we see that if the signal integration time is increased by a factor of ten to 600 seconds the counting statistics improve significantly for both 0°C and 25°C and now there is a statistically significant difference between channel 70-3 and background for both operation temperatures.

A quantitative model relating the specified luminous flux of a source to the signal output of the CCD camera was formulated. A valid model is desirable both to confirm that the prototype was functioning as expected and also to develop a predictive method for determining signal levels in future work. EQUATION 1 represents the model.

$$N_c = [F] \times [T] \times [\Omega] \times [1 + R_s] \times [T_{cl}] \times [T_o] \times [QE] \times [C_{A/D}]$$

[1]

Where:

N_c = Total digital counts from the CCD image collected in integration time T.

F = Photon luminous flux in photons per second per sterradian.

T = Signal integration or sampling time in seconds.

Ω = Collection solid angle of the optics collecting the luminescence signal. The value of Ω is calculated from

the f# of the cameras effective aperature, $\Omega = \pi / [4(f\#)^2]$ and $\Omega = 0.049$ sterradians for and f# of 4.0

R_s = Fraction of luminescence photons redirected back toward the collection optics via reflection. R_s is

assumed to be zero for the optical configuration utilizing the Biolink reference standards.

T_{cl} = Fraction of photons transmitted by the collection optics, T_{cl} is estimated to be ≈ 0.9

T_o = Fraction of photons transmitted by all the other optics in the camera, i.e., the CCD window, the sample

chamber window and the window on the camera head. T_o is estimated to be ≈ 0.9

QE = The quantum efficiency of converting photons from the Biolink source wavelength to photo-electrons

in each well of the silicon CCD. This value is 0.4 photo-electrons per incident photon and is provided

by the camera specifications for light at 540 nm (the λ_{MAX} for the Biolink™ 濤).

$C_{A/D}$ = This number is also provided by the camera specifications and depends on the CCD circuit design

electronics. It represents the number of digital counts arising from each photo-electron created.

This number is 0.43 digital counts per photo-electron for the ST71 camera.

Biolink™ 濤 channels 82-1, 82-3 and 70-1 were used as sources of photon flux and the ST71 integration time was one second. The CCD was operated at 0°C and the collection lens aperature was set at f/4. The decay time normalized signal intensities versus the measured results are shown in TABLE IX below.

TABLE IX A Summary of the Measured and Calculated Digital Signals for Three Biolink Reference Standards

<u>Biolink™ 濤 Channel Measured</u>	<u>Measured Total Digital Counts/s</u>	<u>Calculated Total Digital Counts/s</u>	<u>Ratio C a l c u l a t e d /</u>
82-1	1,166,000	444×10^6	381
82-3	20,500	6.6×10^6	322

TABLE IX shows very poor agreement between the quoted and measured photon digital counts and there is considerable variation in the differences observed for the three Biolink™ channels. A measurement of the photon flux from each of the 15 Biolink™ channels indicated that the ratio of the measured intensities to the quoted decay time corrected intensities was often considerably different. Numerous attempts to contact the manufacturer in England met with no response. Suspecting that the quality control of the reference standards was in doubt we employed a second light standard which is sold by a luminometer company (Turner Designs, Inc.). This luminometer standard is manufactured by TEST-ER, Inc. and consists of 1μCurie of ¹⁴C as palmitic acid in 0.25 ml of ULTIMA Gold™ liquid scintillator (Packard BioScience BV, Netherlands) sealed in a small glass vial with a flat bottom. The glass vial in turn is placed inside a silvered parabolic reflector which serves to re-direct a considerable fraction of the light down towards the bottom of the vial. ¹⁴C decays to ¹⁴N plus a β-particle which interacts with the scintillator to produce photons with a wavelength of 400 – 460 nm. The silicon of the CCD has a quantum efficiency of about 10% at the center wavelength of the scintillator center wavelength.

The isotropic (4π steradians) photon flux from a 1μCurie source containing the 90% efficient scintillator is calculated as:

$$F = [3.7 \times 10^4 \text{ disintegrations/s}] \times [0.9 \text{ photons/disintegration}] / 4\pi \text{ steradians} \\ = 2,650 \text{ photons/s/steradian}$$

Equation [1] was again utilized with an integration time (T) of 600 seconds and the QE for Silicon at a λ_{MAX} of 430 nm being 10%. All of the other values were essentially the same as before except Rs was now estimated to be on the order of 9. The TEST-OR sample was placed on the glass window of the sample chamber and the CCD camera took one 600 second, dark background subtracted image. The total measured signal from the standard was 25,900 digital counts. The calculated total number of photons was 27,600 digital counts – a value in good agreement with the calculated value. All of the parameters in Equation [1] are known or estimated quite accurately except the value of Rs. It is conceivable that it is as great as 10, but more likely that it is closer to 4 – 5.

The signal linearity and detection threshold of the ST7I-based prototype analyzer was compared to that of a Turner Design PMT based photon counting luminometer (Model 20/20) by determining standard calibration curves for both instruments, i.e., background subtracted signal versus ATP concentration. The reagent cocktail used for both assays was as follows: 1 milli-molar luciferin, 10 milli-molar Mg⁺⁺ (a co-factor for luciferase), 0.5 mg/ml bovine serum albumin to passivate surfaces and prevent adsorption and denaturation of luciferase and firefly luciferase at 12 micro-molar concentration. The ATP concentration range

was 1 nano-molar to 10 micro-molar. All reagents were in 0.45 M glycyl-glycine buffer at pH 7.8. The prototype had the provision to analyze one 350 μL capacity microwell placed where the biosensor would normally be. Fifty μL of albumin, luciferin, Mg^{++} concentration was first added to the microwell followed by 10 μL of luciferase concentrate. Then 40 μL of the sample ATP concentration was added and thoroughly mixed via micro-pipet and the sample chamber lid was closed. The CCD bioluminescence signal was integrated from a time period of $T=10\text{ s}$ to $T=70\text{ s}$ following the addition of ATP sample. A 60 s dark thermal background signal was subtracted from the CCD data and the average signal from a 31×31 pixel array comprising the image of the bioluminescence in the microwell was recorded. The prototype CCD chip was operated at 25°C .

A very similar sampling approach was used with the luminometer wherein the ATP solution was auto injected into the luminometer sample cuvette where it mixed with the pre-added luciferase, luciferin, albumin and Mg^{++} concentrate. The peak signal "flash" was background subtracted (0 ATP concentration) and recorded. The standard curves obtained via these protocols are shown in FIGURE 8.. The luminometer was able to detect one nanomolar ATP and had a very linear response over the ATP analyte range (regression analysis correlation coefficient, $r=0.9998$). The ST7I prototype had a minimum detection threshold of about 10 nanomolar ATP and the linearity was not quite as good particularly at the high ATP concentration range of 5-10 micromolar ($r=0.995$). The non-linearity at high ATP is expected. The better sensitivity of the luminometer is understandable considering that it employs a photo-multiplier tube and photon counting to detect the bioluminescence.

Characterization of Analyzer-Biosensor System

Signal uniformity was determined for the four holes of the biosensor without any wicks present. An electroluminescent light source (75 mm square) was placed over the top of the biosensor and an image was taken of the transmitted light. Total background subtracted signal was determined for the full image of each hole. Signal levels were about 36,000 digital counts. The analysis was repeated in triplicate. Coefficients of variation based on the means and two sigma standard deviations were determined and compared for all four holes in a given run and for each hole in three runs. In all cases the coefficients of variation ranged from 2-3 % which suggested very uniform hole illumination.

All wicks were cut reproducibly and precisely to a length of 6 mm using a mitre box type of cutting fixture that was machined to have a cutting slot for a razor blade at 6.0 mm. All wicks utilized were from the same batch for optimal material reproducibility. There was, however, some variability in the bioluminescent signal as a function of time after reagent was applied sequentially to the four wicks. This is illustrated in FIGURE N where the bioluminescent reagents were mixed and immediately applied sequentially to the wicks. The ATP concentration was 10 millimolar. Concentrations of other reagents were as previously described. Sixty second exposures were taken periodically over a period of 20 minutes.

Note that the average signal intensity is quite variable for the four wicks and begins in the 4,000-8,000 digital range. There is a progressive loss of bioluminescence over the 20 minute period, but there is considerable wick to wick variation with the wick to receive the sample first having the lower signal overall and the wick which received the sample last (fourth wick) having the highest signal overall. What is happening is that the concentration of luciferase (12 micromolar) is quite high relative to the concentration of luciferin (1 millimolar). The result is a very brief (tens of milliseconds) flash of bioluminescence followed by a rather rapid decay in light emission as the ATP and luciferin are consumed. Even though the time required to apply reagents to four wicks after mixing is only about 30 seconds there were significant variations in signal in each channel. Since sample in all four channels came from the same batch after mixing it is hypothesized that even short exposure time differences to the high surface area of the polyester wicks is causing considerable detrimental effects on the resultant bioluminescence. Attempts to passivate the fiber surfaces with pre-adsorbed bovine serum albumin and washing the Triton X100 detergent off the fibers had no significant improvement. The solution was to cover the four channels with a S & S 903 paper reagent sample reservoir which served to deliver uniform amounts of the liquid sample to each of the wicks simultaneously. The result was a much more uniform delivery of sample to each of the four channels simultaneously. This is shown in FIGURE NA.

FIGURE P shows the standard curve for ATP derived using the ST7I based prototype and the four channel biosensor.

3. Summary of the Phase I Feasibility Study

The Specific Aims of this Phase I project were accomplished. Three CCD camera systems were evaluated for use in a functional, bench top analyzer prototype. The prototype was constructed and characterized. A new, smaller, six channel biosensor was constructed which could be used in the prototype for the determination of ATP. Evaluation of the analyzer-biosensor system indicated a linear relationship between ATP concentration and CCD signal with good precision over a detection range of 0.1 micromolar to 10 millimolar. This work paves the way to a comprehensive research and development effort to produce functional engineering prototypes of the analyzer and the biosensor. The detection of ATP in the concentration range of 10 micromolar to 10 millimolar is feasible even when the CCD camera is operated at room temperature. A specification for the functional engineering prototype system is detailed in Section B (Significance and Specifications).

Experimental Design and Methods

As previously noted, the CCD camera of choice was the ST7I with a Kodak KAF-0400 CCD chip. Characterization of this camera at 0°C versus 25°C showed that room temperature operation was definitely feasible. If it were necessary to use a **thermo-electric (TE)** cooler to cool the CCD chip to 0°C the

added power consumption would foreclose the possibility of a battery powered, hand held device due to the need for both high power to cool the CCD and a large surface area heat exchanger that would make the device too large and heavy to hold. Finally, the TE cooler and fan would add significantly to a loss of reliability and the overall mechanical design would become at least twice as complicated and expensive. Certainly for point of care sites where a small analyzer sitting on a counter top is acceptable TE cooling could be implemented with a concomitant improvement in sensitivity. However, the focus of our continued development effort is on a hand held analyzer and we envision no serious limits to ATP detection in the range of 10 micro-molar to 10 milli-molar.

Prior to this Phase I CCD project and the employment of Dr. Van Wagenen (the PI) our expertise and R&D efforts were in the area of protein engineering and biosensor biochemistry. We now know that a quantitative analyzer is a necessary component of a successful proof of feasibility luminescence assay. We do not, however, have sufficient in house engineering resources (hardware, electrical, and software design) to continue the development of our CCD based luminescence analyzer. The obvious solution is to subcontract the development work out to a group of development engineers that have had many years of experience commercializing medical devices and disposables. We have chosen a local group (**ECLIPSE Product Development, Inc.**) to collaborate with during this project because of their experience in the design of both disposable and medical devices. ECLIPSE employee, Mark Wood has had experience in the development of two families of monitoring instrumentation which employed CCD array cameras. We will subcontract a considerable amount of the engineering work to ECLIPSE while we focus on device evaluations and refinement of the disposable design.

DESIGN PHILOSOPHY

The requirements of this design call for a low cost, handheld, multi-channel analyzer having a modem or wireless communication capability for networking data to a central medical site. FIGURE 11 illustrates our approach which consists of three specific functional blocks. This Phase II effort focuses on **Block 1** which contains the proprietary and custom portion of the design, i.e., the embedded CCD detector chip that is needed for sensing the luminescence. The CCD detector electronics provide for the low noise read-out of the CCD detector, signal amplification, analog to digital conversion, dynamic configuration of the CCD array, automatic detector alignment, data storage, data analysis via implementation of analytical algorithms and serial or parallel communications to the host computer. Precise and synchronous timings are provided by an internal Time Processor Unit (TPU). The TPU is internal to the MC68332. The TPU simplifies the design by eliminating the need for additional digital hardware to generate time control signals for the CCD.

Block 2 employs an existing **Personal Digital Assistant or PDA** such as a 3COM Palm Pilot or a Handspring Visor to provide an inexpensive graphical user interface and serial communications port (Palm Pilot) or parallel communication port (Visor). The PDA provides a two way communication link connecting the user and a centralized data base. An abundance of application and development software already exists for such PDAs. At least one PDA (the 3COM Palm VII) is now available with built in wireless networking capability and several PDAs now have attachable modems. As the state of the PDA art continues to rapidly advance, it is expected that costs will decrease as performance and capability increase. By building on the efforts of thousands of software developers and utilizing applications and development tools

already available, a tremendous advantage can be had in time to market and overall cost of development. Future design changes are also made at a fraction of the time and cost associated with proprietary software and hardware. Additional benefits are gained in user satisfaction by providing an interface that millions of users already own and are familiar with. Finally, the PDA can be utilized for other applications as well.

Block 3 of FIGURE 11 represents the networked server system at a remote site that has much greater processing capability for data analysis, trending, record keeping, etc. and networking via complex applications software that also serves a variety of other needs.

The proprietary and custom portion of the design i.e. the embedded CCD detector is required for the specific hardware requirements of this application. If design changes are made in the proprietary hardware design, the user interface will nevertheless remain very much the same, having the same look and feel, but with possibly somewhat different functionality. Custom additions are readily implemented with available low cost rapid application development (RAD) tools. In addition to the user interface support, it is expected that a flood of networking application software will be available in the near future. And, while wireless IP networking services appear rather expensive at present, the future for mobile networked devices is compelling. Lower costs and enabling technologies will inevitably emerge to create the vision of pervasive mobile networked computing. Implementation of designs based on standards is imperative to success in this market. Only those products having standard interfaces and protocols will benefit from the vast computing and networking resources of the near future. Our design philosophy then is to interface standard PDA (Palm Pilot) technology into our handheld analyzer. Our design incorporates custom proprietary electronics to interface to standard PDA technology.

Specific Aim 1 - Review and Preparations for Development Phase

At this time, the most likely design scenario employs a Kodak KAF-401E full-frame CCD (6.9 x 4.6 mm) having 768 x 512 pixels (each 9 x 9 μm). This CCD has an enhanced absolute quantum efficiency of 0.55 at 550 nm versus about 0.35 for the Kodak chip we used in Phase I. It also has extremely low dark current (<10 pico-ampl/cm² at room temperature) and it is this specification that makes room temperature operation feasible [reference Kodak]. Currently, we envision a Palm V like handheld computer (PDA) as the user interface. However, both the CCD and PDA technology areas are changing very rapidly and we anticipate considerable additional capability with simultaneous cost reductions before this project is approved and funded. For example, a recent 3COM Palm spin off company called Handspring is now marketing the Visor. This PDA has considerably more applicability to our design and costs fifty percent less than the Palm V.

Consequently, we plan to stay current with the technological developments in these fields so that when we are notified of funding we can immediately begin a thorough review of the design and all of the time critical hardware options and software development tools choices. We will first conduct a review of the **device specification** since this will guide the design effort. We anticipate minimal change in the device specification, but one area that will require additional refinement will be the design of the actual user interface on the PDA screen. Following the final decisions regarding device specifications and user interface, we will formulate a **design specification** that documents how the analyzer will be constructed to accomplish the performance of the device specification. The design document will include all of the hardware choices and a first level design of the software functions and hardware layout. All hardware, software design

tools and equipment will be ordered. **Time Frame:** Month 1

2. Specific Aim 2 - Mechanical Design

Initial mechanical design layout will immediately follow the formulation of the design specification which will include geometry and volume budgets for each of the following key subsystems – batteries, optics, CCD in housing, biosensor chamber, and electronic circuitry. The relationship of the analyzer housing to the PDA will also be defined. This will lead to an overall package design that will include ergonomic considerations appropriate for a handheld device directly attached to a PDA interface. **Time Frame:** Month 1

The primary issue to address first in great detail will be the optical design necessary to collect the emitted luminescence from the biosensor and image it efficiently onto the CCD chip. We plan to evaluate three approaches to luminescence collection and imaging. The first approach will utilize Graded Refractive INDEX (GRIN) lenses oriented in a 3 x 4 array which will correspond to the 3 X 4 array of the 12 channels of the biosensor. GRIN lenses are highly desirable fiber optic like image conduits which provide 1:1 imaging from object (source) to image (CCD detector plane). They are about 1 mm in diameter and several mm long. The distances between the GRIN lens and the object (luminescence) and image (CCD) are typically about 1 mm. This provides for a considerable reduction in the size of the optical system. For comparison, the object distance in the Phase I prototype was about 150 mm. The disadvantage to these small distances is the necessity of using very thin windows to separate the sample and CCD chambers from the GRIN lenses. This approach would not be possible if the CCD required a thermo-electric cooler (non-ambient monitoring) because the chip would have to be several mm from the window to minimize the radiant heat gain.

The second optical design approach will utilize a 3 X 4 array of individual micro-optical lenses from Bern Optics. These refractive lenses will be about 1 mm in diameter and will have short working distances and f#'s in the range of 0.8 to 2.0. The third design approach will employ a collection lens and a focusing lens into a system that will collect the luminescence from 3 X 4 channels of the biosensor and image it onto the 6.9 x 4.5 mm area of the CCD. This approach will also be a 1:1 imaging with an f# of 0.8 – 2.

The various optical designs will be evaluated while other aspects of the mechanical design layout previously noted are being addressed. Thorough evaluation of the three optical designs will require two and possibly three iterations in design and evaluation. Optical design evaluations will utilize the existing ST7I CCD camera operated uncooled at room temperature and with the windows removed when necessary. The final optical design will be selected and factored into the overall design envelope. **Time Frame:** Months 2 – 10.

Package design and interfacing the analyzer to the PDA will also be addressed in this task. When the first round of electrical circuit design is complete and the optical design has been validated the exterior case design will be finalized and prototype cases will be machined from polycarbonate or acrylic. **Time Frame:** Month 10.

Specific Aim 3 - Electrical and Software Design

The CCD detector is comprised of a combination of digital and analog electronics. The major components are depicted schematically in FIGURE 12. The analog components provide level shifting, voltage regulation, a low noise CCD pre-amplifier and analog to digital (A/D) conversion. The digital components provide logic and timing control of the CCD chip, serial communications, data storage and data analysis.

Voltage regulators are required to provide tightly regulated voltages used by the level shifters and the CCD charge sense, low noise pre-amp. This is accomplished using precision reference voltage and low drift op-amps. Voltage level shifting is required to shift from digital logic voltage levels to shift clock voltage levels required by the CCD. This is accomplished by the use of analog

CMOS switches and MOSFET drivers. **Vertical clock drivers** provide charge shifting by a variation of potentials along a row or column. Signal charge is shifted row by row down columns into a horizontal readout register. Charge is then shifted into an output sense node by the **horizontal clock drivers**. The voltages and waveshapes of the clock driver signals must be designed to minimize shift noise. In addition, the vertical clock drivers are designed to drive the CCD with a low dark current “inversion” voltage during signal collection. Driving the CCD into “inversion” results in a reduction of approximately two orders of magnitude in dark current. The output of the CCD sense amp is typically in the micro-volts per electron range. Thus to maintain an acceptable signal to noise ratio it is necessary to amplify the signal with a low noise amplifier before sending it on to an A/D converter. An **analog MUX** is provided to multiplex analog signals that need to be monitored. In addition to the CCD output it will be desirable to monitor voltages levels related to battery life and ambient temperature levels.

The A/D converter is selected based on dynamic range, cost and power dissipation. Dynamic range is determined by resolution and input noise. Low cost 16 bit AD converters are commercially available having low input noise, fast conversion, low power dissipation and simple read-out. These are the logical choice for this application. The **68332 micro-controller** controls all aspects of operation of the CCD detector. It controls CCD readout, AD conversion, data storage and serial communications. The 68332 contains a **Time Processor Unit (TPU)** for generating complex timing and control signals. It is ideal for generating CCD shift clocks and synchronizing readout with AD conversion. The 68332 contains an **RS232 serial data communications port** for communications to a PDA, desktop PC or modem. The 68332 also contains a built in **Background Debug Module (BDM)** for rapid in circuit debugging of code. The BDM enables code to run on the application hardware while enabling control over operation of the CPU during debug sessions.

MARK – I DID NOT CHANGE MUCH OF THIS BECAUSE SOME OF IT WILL PROBABLY CHANGE GIVEN THE PGA DESIGN APPROACH. PLEASE CHANGE ACCORDINGLY. AND CAN YOU PLEASE REDUCE THIS TO WRITTEN TEXT WITH 1-2 SENTENCES OF EXPLANATION AND DETAIL RATHER THAN OUTLINE FORM? THANKS

Detailed Breakdown of Design Tasks

Block 1

Hardware Design

Analog Circuit Design

- Design voltage regulators for low power battery operation

- Review selection of amplifiers for lower power single supply types

Select preamp for optimum power noise tradeoff.

Digital Circuit Design

Design for small footprint FLASH and SRAM

Review use of PDA for containment of boot code.

Design MC68332 using 32Khz crystal clock

Board Layout

Optimize for grounding and low noise while working to reduce cost and board size

Board Build and Assembly

Contract for “hand stuffed” prototypes

Board Testing

Boot up digital electronics using MC68332 BDM development tool

Fix hardware bugs

Get serial communications up and running with PC or handheld

Generate timings for CCD read-out

Debug analog electronics – test voltage levels, drivers, waveshapes etc.

Software Design Tasks

Tools Procurement and Maintenance

Review available software development tools

C/C++ compilers

Support for 68332.

Ease of use.

Compatibility with available operating systems and debuggers.

Debugger

Support for 68332

Features

Operating system

Support for 68332

Memory management

Interrupt processing

Purchase Tools

Install Tools

Configure Tools for board design

Boot Code

Write boot code in assembly for cold boot (power on) from FLASH memory

Serial Communications

Define protocol, command set and status reporting

Implement communications protocol

Test with PDA

CCD Timing and Control

Program TPU for read-out timings

Define types of CCD scanning

Implement software state machine to handle variations in scanning

- Auto Alignment and Calibration
 - Define alignment procedure
 - Capture image
 - Implement software reference locator
 - Determine relative position of signal sample pixels
- Data Analysis and Formatting
 - Define areas of interest
 - Define binning or integration of signal areas
- Prediction Algorithms
 - Define prediction algorithm
 - Implement algorithm

Block 2

Hardware Design Tasks

- Serial Connector
 - Design hardware connector to adapt to PDA serial port

Software Design Tasks

- Serial Communications
 - Define protocol
 - Implement protocol using Palm API
 - Define command interface
 - Link command interface to user interface
 - Test commands with user inputs
- Networking Applications
 - Define basic application protocol
 - Embed in TCP/IP using sockets API
 - Test using wireless networking to remote server
- Graphical User Interface
 - Define look and feel
 - Define user generated events
 - Determine event processing
 - Define data entry
 - Define user prompts and forms
 - Implement user controls, events, data entry
 - Connect user inputs to CCD detector hardware
 - Verify communications
 - Test for random user inputs generating random events
- Data Storage and Management
 - Define data structure
 - Define purpose for data
 - Determine visual display of data i.e. graphs, plots etc
 - Define user access to data
 - Define file formats

Block 3

Software Design Tasks

Networking Applications

Define simple protocol for communications with PDA using TCP/IP

Write server side scripts to respond to PDA client requests

Test with wireless IP modem connected to PDA

Time Frame: Months 2-10

4. Specific Aim 4 - First Round Prototype Evaluation

Time Frame: Month 11 Construct Prototypes

Time Frame: Months 12-15 Evaluate prototypes

5. Specific Aim 5 - Hardware and Software Design Refinement

Time Frame: Months 16- 20

6. Specific Aim 6 - Biosensor Redesign

The existing six channel biosensor has a simple buffer solution sample volume of 20 μL /channel. To attain a 12 channel design with a total maximum blood sample volume of $< 100\mu\text{L}$ the volume of each channel will have to be reduced by a factor of ten to about 2 μL . For a blood hematocrit range of 30% to 60% a 100 μL blood sample would have a sample plasma volume range of 30-60 μL . Our proposed design is illustrated in FIGURE 13. A commercially available blood separation membrane () will be utilized to retain blood cells on the sample side while allowing plasma to wick through the pore structure and re-hydrate the lyophilized contents of each channel. Each channel on the biosensor will be 1 mm in diameter and 2.5 mm deep and will have a volume of 2.0 μL for a total sample volume of 24 μL . The remaining plasma volume will serve to fill pore space in the blood separation membrane with some excess left over depending upon the actual hematocrit of the blood sample.

FIGURE 13 depicts the proposed biosensor design. The main body of the biosensor will be black acrylic or polycarbonate. In the initial prototypes, the 1 mm diameter channel holes will be drilled in a 4 x 3 array on 1.5 mm center distances on the flat bottom of a milled indentation that serves to both contain the blood sample and also serves as an attachment surface for the blood separation membrane. A 0.25 mm polystyrene or polycarbonate window will be ultrasonically welded to the CCD detector side of the biosensor to form a container for the bioluminescent reagents. At this time our bioluminescent reagents are preserved and stabilized with the following components: (1) 0.45 M glycyl glycine buffer (pH 7.8), (2) 1 mM EDTA, (3) 1mM dithiothreitol, (4) 10 mM MgSO_4 , (5) 1 mg/ml of bovine serum albumin, (6) 1 wt% sucrose, and (7) 1 wt% Dextran T-40. The actual bioluminescent molecules (ATP, FMN, bacterial and firefly luciferase, Oxidoreductase, etc.) are added to the preservative reagents, mixed thoroughly and added to each channel of the pre-chilled biosensor. The biosensor and reagents are rapidly frozen to -70°C followed by a two stage lyophilization process. The first stage of lyophilization proceeds for 24 hours at -50°C and < 100 mTorr of pressure. The second stage of lyophilization proceeds for an additional 24 hours at $+30^\circ\text{C}$ and < 100 mTorr of pressure. Air is then re-admitted to the lyophilization chamber, the biosensors are removed and the blood separation membrane is added to seal the dried reagents in place. Each completed biosensor is then stored in a black plastic container with a gas tight lid that also contains a desiccant and a humidity indicator membrane. Our experience to date with firefly luciferase indicates that this approach to preservation can preserve more than half the enzymatic bioluminescent

activity for a minimum of six months.

Time Frame: Months 2-10 and 16-20

Specific Aim 7 - Second Round Prototype Evaluation

Time Frame: Months 20-24

8. Specific Aim 8 - CMOS Image Sensors as Alternative to CCD Image Sensors

Complementary Metal Oxide Semiconductor (CMOS) image sensors promise to offer significant advantages over CCD image sensors. The CMOS technology requires only one lead and a single voltage while CCDs require three leads, three different voltages and three stabilized power supplies. CMOS imaging sensors require only about 10% of the power required by a CCD. And of most importance, the CMOS architecture is made with the same equipment and integrated circuit technology used to make other integrated circuits. This means that the CMOS sensor can be integrated right on to the same chip containing all of the support circuitry. There is a tremendous effort by multi-national corporations (Toshiba, Kodak, etc.) and small startup companies to refine CMOS technology for use in digital cameras, computers and portable videophones. This is because CMOS offers very low power consumption (portability), smaller pixel size (better resolution) and the potential for huge cost reductions (only a few dollars) compared to CCDs. CMOS chips do still currently have some problems. The most serious one being a generally higher noise per pixel, however, improvements in reliability and quality are still necessary for broad commercialization. We are not aware of any efforts to develop cooled CMOS imagers. CCDs while still have the advantage here for some time.

We plan to stay current with the commercial availability of CMOS imaging arrays and during the second year of this project we will obtain the most appropriate prototype for in house evaluation. First, the performance of the CMOS camera will be compared to that of the ST7I camera in our Phase I prototype. The most important metrics to evaluate will be signal to noise ratio, minimum detection threshold, linearity and thermal stability. If the CMOS camera appears to be comparable in performance to the ST7I then it will be incorporated into an engineering prototype design and evaluated in comparison to the other prototypes based on the CCD approach. See Specific Aim 4 above for details.

Time Frame: Months 12-24

Human Subjects No human subjects are involved in this Phase II project.

Vertebrate Animals No vertebrate animals are involved in this Phase II project.

Consultants

No additional consultants are proposed for this development project. We will, however, rely considerably on the expertise of our Scientific Advisory Board members and Dr. Joe Andrade the founder, President, and CEO of Protein Solutions, Inc. Joe has worked extensively with proteins, enzymes, and antibodies for the past 25 years, focusing his efforts on elucidating their behavior at surfaces and interfaces. Joe will be available to assist and consult in the areas of interfacial biochemistry, bioluminescence, and biosensor expertise where required. In addition to Dr. Andrade, our strong Scientific Advisor Board will continue to serve in an advisory and consulting capacity with reimbursement from other sources. The board members are as follows:

Dr. Woody Hastings – Professor of Biology at Harvard University. Dr. Hasting is internationally recognized for his basic research on bioluminescence.

Dr. Vladimir Hlady – associate Professor of Bioengineering at the University of Utah. Dr. Hlady is an expert on the study of proteins at surfaces using interfacial fluorescence spectroscopy in conjunction with CCD detectors.

Dr. Henry Kopecek – Professor of pharmaceuticals and Bioengineering at the University of Utah. Dr. Kopecek is an internationally recognized authority on hydrogels and related polymers for drug delivery and biocompatibility.

Dr. Larry Kricka – Director of the General Chemistry Lab and Professor of Pathology and Laboratory Medicine at the University of Pennsylvania. Dr. Kricka is internationally recognized for his work on applying both bioluminescence and chemiluminescence to clinical chemistry.

Dr. Russell Stewart – Assistant Professor of Bioengineering at the University of Utah. Dr. Stewart is an expert on recombinant techniques for the synthesis and study of luciferases and motor proteins.

Our consultants will be reimbursed for their services from other monetary resources available to the company.

Consortium Arrangements

Literature

Andrade, J.D., Wang, C.Y., Min, D.-J., Eu, C., Van Wagenen, R., and Scheer, R., "Toward Dollar Devices for Measuring Metabolic Biochemistry", in S.P. Sawan and G. Manivannan, eds., Anti-Microbial, Anti-Infective Materials, Technomic Publishing (1999) pp. 317-329.

Brolin, S. and Wettermark, G., Bioluminescence Analysis, Weinheim Publishing (1992).

Eu, J.-Y., Wang, C.-Y., and Andrade, J.D., "Homogeneous Bioluminescence Assay for Galactosuria: Interference and Kinetic Analysis", Anal. Biochem., **271** 168-176 (1999).

Leaback, D.H., "Easy-To-Use Light Standards as Aids to Luminometry", in A.A. Szalay, L.J. Kricka and P. Stanley eds., Bioluminescence and Chemiluminescence, John Wiley & Sons Publishing (1993) pp. 33-37.

Min, D.J. and Andrade, J.D., "Preliminary Study of the Optimum Conditions for a Lactate Sensor based on Bacterial Bioluminescence" in J.W. Hastings, L.J. Kricka, and P.E. Stanley eds., Bioluminescence and Chemiluminescence: Molecular Reporting with Photons, John Wiley & Sons Publishing (1997) pp. 275-278.

Min, D.J., Andrade, J.D., and Stewart, R.J., "Specific Immobilization of in Vivo Biotinylated Bacterial Luciferase and FMN:NAD(P)H Oxidoreductase", Anal.Biochem., 270 133-139 (1999).

Dr. Geoffrey Cheung
National Center for Research Resources

May 2, 2000

Re: Response to IRG Summary Statement of R44 RR 13087-02

Dear Dr. Cheung,

Thank you for your letter of Mar. 28, signed by Dr. Beitins, and the Summary Statement.

Although we are pleased with the complimentary aspects of the Summary Statement, **we must respond to a number of perspectives, opinions, and conclusions which are not warranted and require correction:**

Critique # 1, pp. 2-3:

There was concern that the "...experimentally simple..." format proposed in Phase I was being replaced by a more complex approach. The situation is just the opposite. The original spatial gradient format is the more complex and difficult to implement. The Phase II application proposes to use discrete well-based individual analyte channels which are easier to implement and generally more sensitive and reliable than the spatial gradient format.

There was concern about the "...efficacy of the proposed assay formats..." As specific analytes and their assays were not the focus of the proposal, we did not allocate much of the limited space to their discussion in the proposal. The assays under development have target CVs in the +/- 3 to +/- 5 % range with a one year shelf life.

The reviewer stated that "...there is substantial competition in the commercial realm for automated clinical analyzers." True, but our goal is to produce a multi-analyte HOME analyzer. There is little commercial interest in this area (except for home glucose measurements), largely because the other analytes of interest for home monitoring require highly sensitive, but inexpensive and easy to use, monitors. Our goal is home use – not the clinical lab or clinic/hospital applications.

The reviewer was concerned about "...single target assay formats..." We have not proposed single target assays – rather we propose panels, which require a multi-analyte, multi-channel instrument.

Critique # 2, p-3,4:

The reviewer claims that "...there are a lot of competing analyzers for these and other analytes." No, there are not. HOME monitors for creatinine and lactate are not available. There is a lactate device used by coaches and trainers, but it is too expensive for home use. Creatinine is available for some critical care/ point of care devices, but not for home use (as is needed by kidney transplant recipients). The ATP and NADH channels are reference channels, as the creatinine assay is based on ATP bioluminescence while lactate couples to NADH bioluminescence. The 4 analytes proposed in the Phase II application are thus reference and model analytes. Their successful development will enable expansion to a wide range of other analytes. The analytes proposed and the hand-held portable luminometer instrument should be considered an enabling technology.

"The only weakness in this proposal is the absence of a detailed Phase III plan." Yes, we

agree. We are in a “chicken and egg” situation. We need to demonstrate a hand-held, inexpensive, easy to use luminometer in order to generate investment and commercial interest in the various home assay panels.

Since the proposal was submitted, we have completed an extensive marketing analysis, concluding that an optimal initial application is the monitoring, in their home environments, of kidney transplant recipients, as well as patients on hemodialysis. Our plan is to work with corporate partners focused in specific clinical areas. We have discussions pending in May and June with several such potential partners in the transplant and hemodialysis areas.

There was concern that we have “...been in business for 12 years...” and with our “...will to commercialize...” Our first 7 years were as a science education products company (science kits). We have focused on biosensors for the past 4 1/2 years. We have a strong will to commercialize home sensors and monitors for chronic disease management.

Summary:

Much of the Summary Statement is highly complimentary and positive. Most of the critique is based on perspectives and opinions which are not warranted, as we have noted above. Finally, there is indeed an important and unmet need for sensitive, reliable, multi-analyte bioanalytical devices for the monitoring and management of a range of conditions, including phenylketonuria (PKU), galactosemia, kidney transplant function, and hemodialysis. These areas are not as profitable and commercially attractive as diabetes and glucose monitoring. They are small, niche markets, of little commercial interest to larger firms or to traditional investors. These are needed areas, however; these patients are underserved.

Finally – we sincerely hope that the staff will see fit to recommend funding of this Phase II application, largely on the basis of societal need. The instrument proposed will be applicable to many different “orphan” needs and populations.

Thank you for the opportunity to provide this needed input.

Sincerely,

RVW, etc